Journal of
Materials Chemistry C

Accepted Manuscript

This article can be cited before page numbers have been issued, to do this please use: X. Song, W. Zhang, X. Li, H. Jiang, C. Shen and W. Zhu, *J. Mater. Chem. C*, 2016, DOI: 10.1039/C6TC03418G.

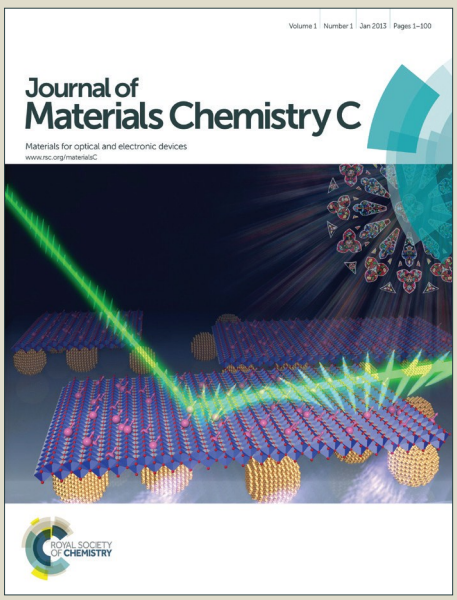

ROYAL SOCIETY OF CHEMISTRY

www.rsc.org/materialsC

View Article Online
DOI: 10.1039/C6TC03418G

Journal Name

ARTICLE

Influence of ethynyl position on benzothiadiazole based D-A-π-A dye-sensitized solar cells: spectral response and photovoltage performance†

Received 00th January 20xx,
Accepted 00th January 20xx

DOI: 10.1039/x0xx00000x

www.rsc.org/

Xiongrong Song,[a] Weiwei Zhang,[a] Xin Li,[b] Huiyun Jiang,[a] Chao Shen[a] and Wei-Hong Zhu*[a]

Ethynyl group has been widely employed in dye-sensitized solar cells (DSSCs) as an efficient π-spacer to prolong the conjugation and promote electronic coupling at the interface of TiO_2 films. However, the systematic study of ethynyl position on metal-free organic sensitizers remains relatively blank. Herein we report indoline-based organic dyes bearing an ethynyl group in different position of D-A-π-A featured organic dyes. Based on the reference dye **D1**, we insert an ethynyl unit in either the left or right side of benzothiadiazole to construct two novel dyes **D2** and **D3**. As found, inserting an ethynyl unit to the side of anchoring group obtains higher molar extinction coefficient with red shift in absorption band. Interestingly, **D2** and **D3** display better photovoltaic performance with respect to **D1**. Especially, **D3** exhibits an over 90 mV enhanced open-circuit voltage (V_{OC}) than **D2** owing to longer electron lifetime and slower charge recombination. With this incredible increase of V_{OC}, **D3** bestows a high efficiency of 7.13% with respect to **D1** and **D2**. Coadsorption strategy are exploited for further improving the cell behaviour. As result, cosensitization with a long-wavelength-responsive dye **WS-2** is demonstrated to efficiently compensate the light-harvesting, achieving an excellent efficiency of 9.83% in the iodine electrolyte. This work has paved a useful and practical way for molecular engineering in D-A-π-A featured metal-free organic dyes.

1 Introduction

Recently, tremendous research has endeavored in exploiting solar energy for the strategy of renewable energy sustainable development.[1] As an effective utilization of solar energy with low cost and facile fabrication, dye-sensitized solar cells have gained extensive attention.[2-3] Here the structural engineering of sensitizing dyes plays a vital role, which can rationally affect the performance of fabricated solar cells by influencing the molecular planarity, light-harvesting ability and molecular interaction.[4-21]

Since Diau et al. reported "push-pull" porphyrin dyes by incorporating ethynylcoboxyphenyl as anchoring group, ethynyl unit has been widely exploited to link with porphyrin for constructing new kinds of sensitizers, which can well promote strong electronic coupling at the interface of TiO_2 films and broaden the light-harvesting region, resulting in a better photovoltaic performances.[22-31] For example, Grätzel et al. has reported two ethynyl-containing porphyrin sensitizers SM315 and SM371, especially achieving a record efficiency of 13% in 2014.[22] Xie et al. also successfully inserted multiple triple bonds to porphyrin sensitizers, along with cosensitization strategy to achieve a high efficiency of 10.45% in iodine electrolyte.[27b] More recently, Wang et al. also introduced ethynyl group to metal-free donor-acceptor dye, realizing a remarkable power conversion efficiency of 12.5%.[26] However, the systematic study of ethynyl position on metal-free organic sensitizers remains relatively blank.[32]

Alternatively, a molecular so-called D-A-π-A model by incorporating an auxiliary acceptor into the π bridge has been demonstrated to be an effective way to decrease the optical band gap, stabilize the electron-rich donor, and improve the dye stability.[33] With the introduction of auxiliary group like benzothiadiazole (BTD), both of metal-free organic dyes and porphyrin dyes show significant promotion in photovoltaic performances.[1b,3a]

With these in mind, we design three novel D-A-π-A featured dyes (Fig. 1). **D1** is an indoline-based D-A-π-A sensitizer featuring BTD group as an auxiliary acceptor and benzoic acid

[a] Shanghai Key Laboratory of Functional Materials Chemistry, Key Laboratory for Advanced Materials and Institute of Fine Chemicals, Collaborative Innovation Center for Coal Based Energy (i-CCE), School of Chemistry and Molecular Engineering, East China University of Science and Technology, Shanghai 200237, P. R. China. E-mail: whzhu@ecust.edu.cn.
[b] Division of Theoretical Chemistry and Biology, School of Biotechnology, KTH Royal Institute of Technology, SE-10691 Stockholm, Sweden.

†Electronic Supplementary Information (ESI) available: Cyclic voltammograms, calculated energy levels, and structural characterization of dyes **D1**, **D2** and **D3**. See DOI: 10.1039/x0xx00000x.

View Article Online
DOI: 10.1039/C6TC03415C

as an anchoring group. The DSSCs fabricated with **D1** displayed a power conversion efficiency (PCE, η) of 6.12%. Based on **D1**, we attempted to insert an ethynyl unit in different sides of BTD group to construct another two novel dyes named **D2** and **D3**, respectively. Both of them performed enhanced efficiencies than **D1**. Interestingly, with a little change in molecular design, **D3** based DSSCs exhibited a great enhancement in photovoltage compared to **D2**, which can be ascribed to the longer electron lifetime of **D3** based devices. Moreover, the cosensitization stragety[34-38] of **D3** with a board absorption spectra **WS-2** was adopted to further improve the photovoltaic performances increasing from 7.13% to 9.83%.

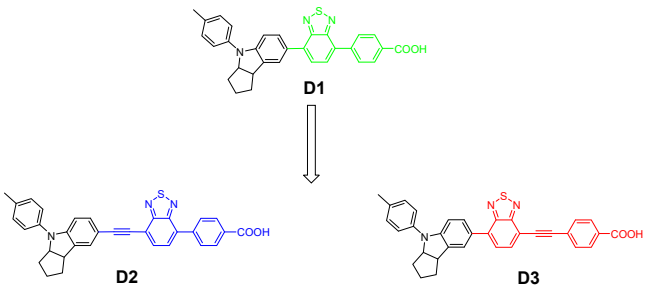

Fig. 1 Chemical structures of dyes **D1**, **D2** and **D3**. Note: Based on **D1**, an ethynyl unit is inserted in different sides of BTD group for taking systematic insight into the ethynyl position effect on metal-free organic sensitizers.

2 Experimental

2.1 Characterization

^{1}H and ^{1}C NMR spectra were obtained with a Bruker AM 400 spectrometer. HR-MS spectra was carried out with a Waters LCT Premier XE spectrometer. The UV-Vis absorption spectra were performed using a model CARY 100 spectrophotometer. The cyclic voltammogram (CV) were tested in dichloromethane with a Versastat II electrochemical workstation (Princeton Applied Research) based on a three electrode system, using Pt as working electrode, Pt wire as counter electrode, and saturated calomel reference electrode (SCE) as reference electrode, respectively.

2.2 Device fabrication and measurements of solar cells

The fabrication of solar cells as well as the relevant preparation of TiO_2 photoanodes (a 6 μm nanoporous layer and a 8 μm scattering layer) and counter electrodes were following the previous work.[10] Each dye dissolved in a mixture solvent ($CHCl_3$:C_2H_5OH = 1:1) was used as a dye sensitized solution with a concentration of 3×10^{-4} M. For single dye sensitized solar cells, the TiO_2 films were dipped in the dye solution for 12 h, rinsed with ethanol and dried. For cosensitization process, the TiO_2 films were firstly immersed in a solution of **WS-2** for 1 h, and then were immersed in a solution of **D3** for 12 h, rinsed with ethanol and dried. The liquid redox electrolyte was made according to reference.[35]

The photocurrent-photovoltage (*I-V*) curves were measured under AM 1.5G simulated solar light using Keithley 2400 Sourcemeter Instruments. The incident photon-to-charge carrier efficiencies (IPCEs) were measured using Newport-74125 system (Newport Instruments). Electrochemical impedance spectroscopy (EIS) was performed for DSSCs using a Zahner IM6e electrochemical workstation, with an alternative sinusoidal perturbation of 5 mV and a frequency range of 0.1 Hz-100 kHz. The original spectra further analyzed by Z-View software.

2.3 Materials and synthesis

Tetrahydrofuran (THF) was refluxed using sodium for dehydration under argon atmosphere before use. All other chemical reagents and solvents were commercially available and used without further purification.

Synthesis of compound 1b. In a 250 mL three-necked flask, bis(pinacolato)diboron (8.3 g, 32.68 mmol), **1a** (1.86 g, 8.65 mmol), KOAc (2 g, 20 mmol) and Pd(dppf)Cl_2 (0.40 g, 0.54 mmol) were dissolved in DMSO (100 mL) under argon. After stirring at 50 °C for 8 h, the mixture was washed with H_2O, dried over anhydrous Na_2SO_4, and evaporated under reduced pressure, the residue was purified on a silica gel column to obtain white powder **1b** (2.0 g, 88%). ^{1}H NMR (400 MHz, $CDCl_3$, *δ*, ppm): 8.02 (d, *J* = 8.4 Hz, 2H), 7.87 (d, *J* = 8.4 Hz, 2H), 3.92 (s, 3H), 1.36 (s, 12H). ^{13}C NMR (100 MHz, $CDCl_3$, *δ*, ppm): 167.15, 134.67, 132.30, 128.60, 84.18, 52.16, 24.89.

Synthesis of compound 1c. In a 250 mL three-necked flask, **1b** (1.0 g, 3.8 mmol), 4,7-dibromobenzo[*c*][1,2,5]thiadiazole (2.28 g, 7.7 mmol) and Pd(PPh_3)$_4$ (230 mg, 0.2 mmol) were dissolved in THF (150 mL), and 2M K_2CO_3 (50 mL) was added. After stirring at 80 °C for 8 h, the mixture was extracted with CH_2Cl_2 and removed under reduced pressure. The residue was purified on a silica gel column to obtain faint yellow solid **1c** (780 mg, 59 %). ^{1}H NMR (400 MHz, $CDCl_3$, *δ*, ppm): 8.20 (d, *J* = 8.4 Hz, 2H), 7.99 (d, *J* = 8.0 Hz, 2H), 7.96 (d, *J* = 7.2 Hz, 1H), 7.64 (d, *J* = 7.6 Hz, 1H), 3.97 (s, 3H). ^{13}C NMR (100 MHz, $CDCl_3$, *δ*, ppm): 166.76, 153.90, 152.87, 140.95, 132.82, 132.19, 130.11, 129.94, 129.16, 128.78, 114.25, 52.31. HRMS–ESI (*m/z*): [M + H]$^+$ Calcd. for ($C_{14}H_{10}BrN_2O_2S$), 348.9646, found: 348.9645.

View Article Online
DOI: 10.1039/C6TC03418G

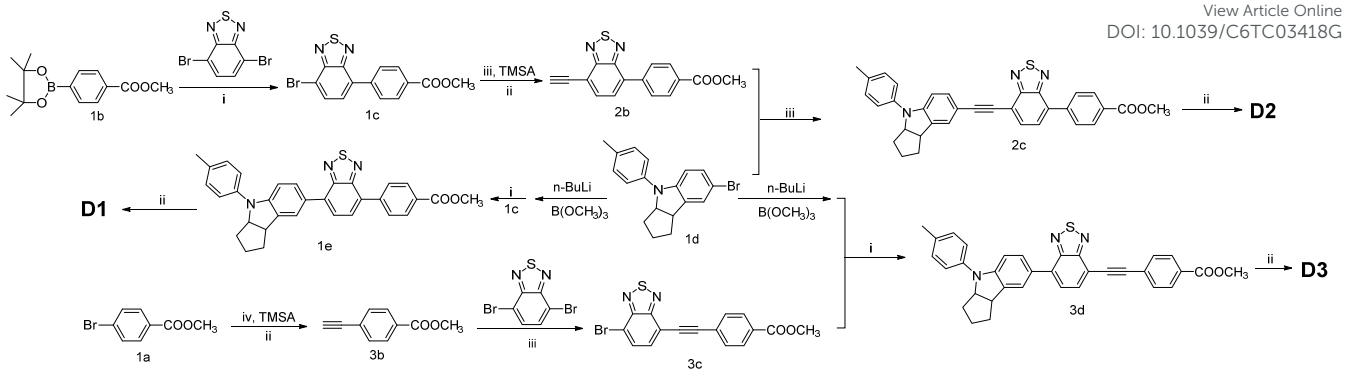

Scheme 1 Synthetic routes to **D1**, **D2** and **D3**: (i) $Pd(PPh_3)_4$, 2M K_2CO_3; (ii) KOH, MeOH, THF, H_2O; (iii) $Pd(PPh_3)_2Cl_2$, CuI, Et_3N.

Synthesis of compound 1e. To a solution of **1d** (470 mg, 1.43 mmol) in dry THF (6 mL) was added *n*-BuLi (0.7 mL, 1.58 mmol) dropwise at -78 °C under argon in dark. After stirring 30 min at -78 °C, $B(OCH_3)_3$ (0.3 mL, 2.1 mmol) was added. The reaction mixture was stirred at the same temperature for 4 h, then gradually warmed up to room temperature and used for the next Suzuki coupling reaction without purification. The unpurified mixture was refluxed with **1c** (566 mg, 1.62 mmol) adding $Pd(PPh_3)_4$ (92 mg, 0.08 mmol) and 2 M K_2CO_3 aqueous solution (30 mL) in THF (100 mL) for 12 h. After cooling, water was added and the reaction mixture was extracted with CH_2Cl_2. The combined organic layer was washed with H_2O and brine, dried over anhydrous Na_2SO_4, and evaporated under reduced pressure. The residue was purified on a silica gel column to obtain red powder **1e** (393 mg, 53%). ^{1}H NMR (400 MHz, $CDCl_3$, δ, ppm): 8.11 (d, J = 8.4 Hz, 2H), 7.98 (d, J = 8.4 Hz, 2H), 7.71 (d, J = 7.2 Hz, 2H), 7.65 (d, J = 7.6 Hz, 2H), 7.16 (d, J = 7.2 Hz, 2H), 7.10 (d, J = 8.4 Hz, 2H), 6.95 (d, J = 8.4 Hz, 1H), 4.79 (m, 1H), 3.88 (m, 4H), 2.27 (s, 3H), 1.97-2.04 (m, 1H), 1.86-1.90 (m, 2H), 1.69-1.78 (m, 1H), 1.49-1.64 (m, 2H). ^{13}C NMR (100 MHz, $CDCl_3$, δ, ppm): 166.99, 154.24, 154.03, 148.67, 142.19, 140.11, 135.39, 134.75, 131.80, 129.84, 129.06, 128.97, 127.02, 126.04, 125.62, 120.42, 107.40, 69.34, 52.20, 45.45, 35.22, 33.73, 29.71, 24.48, 20.83. HRMS–ESI (*m/z*): $[M + H]^+$ Calcd. for ($C_{32}H_{28}N_3O_2S$), 518.1902, found: 518.1902.

Synthesis of dye D1. A mixture of **1e** (300 mg, 0.58 mmol) and KOH (350 mg, 6.2 mmol) in THF (40 mL) and H_2O (6 mL) was refluxed for 12 h under nitrogen. Then, the solvent was removed under reduced pressure. The residue was purified by column chromatography on silica gel to obtain the product as a red powder (219 mg, yield 75 %). ^{1}H NMR (400 MHz, DMSO, δ, ppm): 8.12 (d, J = 6.4 Hz, 4H), 7.99 (d, J = 6.0 Hz, 1H), 7.88 (m, 2H), 7.80 (d, J = 8.0 Hz, 1H), 7.23 (m, 4H), 6.98 (d, J = 8.0 Hz, 1H), 4.93 (m, 1H), 3.92 (m, 1H), 2.30 (s, 3H), 2.08 (m, 1H), 1.81 (m, 3H), 1.64 (m, 1H), 1.40 (m, 1H). ^{13}C NMR (100 MHz, DMSO, δ, ppm): 153.36, 147.71, 139.51, 135.03, 133.40, 130.93, 129.78, 129.43, 129.27, 129.18, 128.94, 128.84, 126.48, 126.05, 125.42, 119.75, 106.80, 68.36, 44.58, 34.87, 33.11, 23.97, 20.38. HRMS–ESI (*m/z*): $[M + H]^+$ Calcd. for ($C_{31}H_{26}N_3O_2S$), 504.1746, found: 504.1751.

Synthesis of compound 2b. In a 250 mL three-necked flask, **1c** (694 mg, 1.99 mmol), CuI (64 mg, 0.34 mmol), $Pd(PPh_3)_2Cl_2$ (100 mg, 0.14 mmol) were dissolved in THF (30 mL) and Et_3N (10 mL) under nitrogen. Then trimethylsilylacetylene (0.8 mL, 5 mmol) was added. After stirring at 50 °C for 24 h, the solvent was removed under reduced pressure, then KOH (150 mg, 2.7 mmol), a few drops of methanol and 30 mL THF were mixed in it and stirred for 30 min at room temperature. Next the organic layer was extracted with CH_2Cl_2 and dried over Na_2SO_4. After the solvent was removed under reduced pressure, the residue was purified on a silica gel column to obtain **2b** (310 mg, yield 53%). ^{1}H NMR (400 MHz, $CDCl_3$, δ, ppm): 8.21 (d, J = 8.4 Hz, 2H), 8.03 (d, J = 8.4 Hz, 2H), 7.91 (d, J = 7.6 Hz, 1H), 7.74 (d, J = 7.6 Hz, 1H), 3.97 (s, 3H), 3.66 (s, 1H). ^{13}C NMR (100 MHz, $CDCl_3$, δ, ppm): 166.76, 155.43, 152.80, 141.06, 134.24, 133.82, 130.21, 129.25, 127.94, 115.51, 84.21, 79.25, 52.31. HRMS–ESI (*m/z*): $[M + H]^+$ Calcd. for ($C_{16}H_{11}N_2O_2S$), 295.0541, found: 295.0538.

Synthesis of compound 2c. **1d** (300 mg, 0.91 mmol), **2b** (250 mg, 0.85 mmol), $Pd(PPh_3)_2Cl_2$ (100 mg, 0.14 mmol), and CuI (40 mg, 0.21 mmol) were placed in a 100 mL three-necked flask, flushed with nitrogen and then charged with dry THF (10 mL) and Et_3N (2 mL). The mixture was stirred at 60 °C for 12 h. Then, the solvent was removed under reduced pressure, and the residue was dissolved in CH_2Cl_2 and dried over Na_2SO_4. After removing the solvent under reduced pressure, the residue was purified on a silica gel column to obtain **2c** (92 mg, 20%). ^{1}H NMR (400 MHz, $CDCl_3$, δ, ppm): 8.20 (d, J = 8.6 Hz, 2H), 8.05 (d, J = 8.6 Hz, 2H), 7.82 (d, J = 7.4 Hz, 1H), 7.74 (d, J = 7.4 Hz, 1H), 7.42 (s, 1H), 7.37 (m, 1H), 7.19 (s, 4H), 6.82 (d, J = 8.4 Hz, 1H), 4.84 (m, 1H), 3.97 (s, 3H), 3.83 (m, 1H), 2.35 (s, 3H), 1.64-2.10 (m, 6H). ^{13}C NMR (100 MHz, $CDCl_3$, δ, ppm): 166.88, 155.30, 153.01, 149.09, 141.57, 139.55, 135.03, 132.42, 132.36, 132.02, 131.60, 129.89, 129.87, 129.77, 129.12, 128.41, 128.38, 120.90, 117.96, 110.91, 106.93, 99.21, 83.72, 69.32, 52.25, 45.13, 35.14, 33.58, 29.71, 24.37, 20.86. HRMS–ESI (*m/z*): $[M + H]^+$ Calcd. for ($C_{34}H_{28}N_3O_2S$), 542.1902, found: 542.1894.

Synthesis of dye D2. A mixture of **2c** (50 mg, 0.09 mmol) and KOH (50 mg, 0.9 mmol) in THF (20 mL) and H_2O (3 mL) was refluxed for 12 h under nitrogen. Then, the solvent was removed under reduced pressure. The residue was purified by

View Article Online
DOI: 10.1039/C6TC03418C

column chromatography on silica gel to get the product as a red powder (25 mg, yield 54%). ^{1}H NMR (400 MHz, DMSO, δ, ppm): 8.13 (m, 4H), 7.95 (m, 2H), 7.36 (s, 1H), 7.30 (d, J = 8.0 Hz, 1H), 7.22 (m, 4H), 6.82 (d, J = 8.4 Hz, 1H), 4.93 (m, 1H), 3.84 (m, 1H), 2.30 (s, 3H), 1.96-2.08 (m, 2H), 1.73-1.81 (m, 2H), 1.36-1.47 (m, 2H). ^{13}C NMR (100 MHz, DMSO, δ, ppm): 167.04, 154.53, 152.33, 148.49, 140.59, 138.77, 135.27, 132.03, 131.80, 131.31, 129.83, 129.47, 129.12, 128.68, 127.82, 120.51, 116.10, 110.03, 106.53, 98.40, 84.06, 68.40, 44.26, 34.90, 32.88, 28.97, 23.90, 20.39. HRMS–ESI (m/z): [M + H]$^+$ Calcd. for ($C_{33}H_{26}N_3O_2S$), 528.1743, found: 528.1746.

Synthesis of compound 3b. In a 250 mL three-necked flask, methyl 4-bromobenzoate (2.0 g, 9.3 mmol), CuI (90 mg, 0.5 mmol), $Pd(PPh_3)_2Cl_2$ (300 mg, 0.42 mmol) were dissolved in THF (100 mL) and Et_3N (30 mL) under nitrogen. Then trimethylsilylacetylene (3.2 mL, 20 mmol) was added. After stirring at 60 °C for 24 h, the solvent was removed under reduced pressure, then KOH (202 mg, 3.6 mmol), a few drops of methanol and 30 mL THF were mixed in it, and stirred for 30 min at room temperature. Next the organic layer was extracted with CH_2Cl_2 and dried over Na_2SO_4. After the solvent was removed under reduced pressure, the residue was purified on a silica gel column to obtain grey powder **3b** (454 mg, yield 30%). ^{1}H NMR (400 MHz, $CDCl_3$, δ, ppm): 8.00 (d, J = 8.5 Hz, 2H), 7.55 (d, J = 8.5 Hz, 2H), 3.92 (s, 3H), 3.23 (s, 1H). ^{13}C NMR (100 MHz, $CDCl_3$, δ, ppm): 166.43, 132.09, 130.12, 129.46, 126.74, 82.79, 80.07, 52.30.

Synthesis of compound 3c. 4,7-dibromobenzo[c][1,2,5]thiadiazole (661 mg, 2.25 mmol), **3b** (300 mg, 1.87 mmol), $Pd(PPh_3)_2Cl_2$ (70 mg, 0.1 mmol), and CuI (22 mg, 0.1 mmol) were placed in a 100 mL three-necked flask, flushed with nitrogen and then charged with dry THF (20 mL) and Et_3N (2 mL). The mixture was stirred at 60 °C for 12 h. Then, the solvent was removed under reduced pressure, and the residue was dissolved in CH_2Cl_2 and dried over Na_2SO_4. After removing the solvent under reduced pressure, the residue was purified on a silica gel column to get yellow solid **3c** (250 mg, 36%). ^{1}H NMR (400 MHz, $CDCl_3$, δ, ppm): 8.07 (d, J = 8.4 Hz, 2H), 7.87 (d, J = 7.2 Hz, 1H), 7.71 (m, 3H), 3.95 (s, 3H). ^{13}C NMR (100 MHz, $CDCl_3$, δ, ppm): 166.44, 166.28, 133.18, 132.47, 131.96, 131.88, 130.29, 129.61, 129.58, 127.00, 116.14, 115.38, 95.76, 87.18, 52.33. HRMS–ESI (m/z): [M + H]$^+$ Calcd. for ($C_{16}H_{10}{}^{79}BrN_2O_2S$), 372.9646, found: 372.9641; [M + H]$^+$ Calcd. for ($C_{16}H_{10}{}^{81}BrN_2O_2S$), 374.9626, found: 374.9644.

Synthesis of compound 3d. To a solution of **1d** (214 mg，0.65 mmol) in dry THF (10 mL) was added n-BuLi (0.4 mL, 0.8 mmol) dropwise at -78 °C under argon in dark. After 30 min of stirring at -78 °C, $B(OCH_3)_3$ (0.2 mL, 1.4 mmol) was added. The reaction mixture was stirred at the same temperature for 4 h, then gradually warmed up to room temperature and used for the next Suzuki coupling reaction without purification. The unpurified mixture was refluxed with **3c** (200 mg, 0.54 mmol) adding $Pd(PPh_3)_4$ (0.1 g, 0.08 mmol) and 2M K_2CO_3 aqueous solution (30 mL) as catalysts in THF (100 mL) for 12 h. After cooling, water was added and the reaction mixture was extracted with CH_2Cl_2. The combined organic layer was washed with H_2O and dried over Na_2SO_4, and evaporated under reduced pressure to obtain red powder **3d** (163 mg, 55%). ^{1}H NMR (400 MHz, $CDCl_3$, δ, ppm): 8.07 (d, J = 8.4 Hz, 2H), 7.87 (d, J = 7.5 Hz, 1H), 7.79 (s, 1H), 7.75 (m, 3H), 7.66 (d, J = 7.5 Hz, 1H), 7.22 (m, 4H), 7.01 (d, J = 8.4 Hz, 1H), 4.88 (t, J = 6.5 Hz, 1H), 3.95 (m, 4H), 2.35 (s, 3H), 2.04-2.15 (m, 1H), 1.93-1.98 (m, 2H), 1.76-1.86 (m, 1H), 1.59-1.72 (m, 2H). ^{13}C NMR (100 MHz, $CDCl_3$, δ, ppm): 166.57, 155.46, 153.30, 148.95, 139.92, 135.71, 135.46, 133.75, 131.99, 131.80, 129.86, 129.77, 129.55, 129.16, 127.71, 126.63, 125.62, 125.44, 120.54, 113.15, 107.35, 94.31, 88.77, 69.35, 52.28, 45.39, 35.25, 33.68, 24.45, 20.85. HRMS–ESI (m/z): [M + H]$^+$ Calcd. for ($C_{34}H_{28}N_3O_2S$), 542.1902, found: 542.1904.

Synthesis of dye D3. A mixture of **3d** (50 mg, 0.09 mmol) and KOH (50 mg, 0.9 mmol) in THF (20 mL) and H_2O (5 mL) was refluxed for 12 h under nitrogen. Then, the solvent was removed under reduced pressure. The residue was purified by column chromatography on silica gel to obtain the product **D3** as a red powder (31 mg, yield 65 %). ^{1}H NMR (400 MHz, DMSO, δ, ppm): 8.02 (dd, J_1 = 8.2 Hz, J_2 = 2.1 Hz, 3H), 7.90 (s, 1H), 7.84 (m, 2H), 7.75 (d, J = 8.2 Hz, 2H), 7.24 (q, J = 8.4 Hz, 4H), 6.96 (d, J = 8.4 Hz, 1H), 4.94 (m, 1H), 3.91 (m, 1H), 2.30 (s, 3H), 2.03-2.15 (m, 1H), 1.77-1.87 (m, 3H), 1.64-1.66 (m, 1H), 1.36-1.47 (m, 1H). ^{13}C NMR (100 MHz, DMSO, δ, ppm): 166.73, 154.81, 152.43, 148.07, 139.31, 135.15, 134.62, 133.99, 131.52, 131.16, 129.81, 129.66, 129.11, 126.28, 126.03, 125.45, 119.94, 111.93, 106.74, 93.86, 88.71, 68.40, 44.53, 34.89, 33.04, 23.94, 20.39. HRMS–ESI (m/z): [M + H]$^+$ Calcd. for ($C_{33}H_{26}N_3O_2S$), 528.1746, found: 528.1746.

Results and discussion

The synthetic routes of dyes **D1** to **D3** are shown in Scheme 1. The common intermediates **1c** and **1d** were synthesized according to the reference.[10,26,27] Dye **D1** was conveniently obtained by the Suzuki-Miyaura coupling reaction of **1c** and **1d**, and then hydrolysis of **1e**. For the ethynyl-containing dye **D2**, we firstly introduced the triple bond to the intermediate **1c** *via* the Sonogashira reaction, and obtained the intermediate **2b**. It was further reacted with **1d** to give the dye precursor **2c**, and eventually gained dye **D2** after hydrolysis. The synthetic procedure of dye **D3** was similar to that of dye **D2**. The only change is that the insertion of triple bond is close to the anchoring group, rather than the neighboring donor.

View Article Online
DOI: 10.1039/C6TC03418G

Table 1 Optical and electrochemical properties of dyes **D1**, **D2** and **D3**.

Dye	λ_{max} [nm][a]	ε [$M^{-1}cm^{-1}$][a]	λ_{max} on TiO_2 [nm][b]	HOMO [V][c] (*vs.* NHE)	E_{0-0} [V][d]	LUMO [V][d] (*vs.* NHE)
D1	484	19900	462	0.87	2.17	-1.30
D2	482	22300	453	0.91	2.18	-1.27
D3	508	25700	474	0.88	2.07	-1.19

[a]Absorption peaks (λ_{max}) and molar extinction coefficients (ε) in CH_2Cl_2. [b]Absorption peaks on 3 μm TiO_2 films. [c]The HOMO was measured in CH_2Cl_2 by cyclic voltammograms (CV), based on a three electrode system, using Pt as working electrode, Pt wire as counter electrode, and saturated calomel reference electrode (SCE) as reference electrode, calibrated with ferrocene as an external reference and converted to NHE by addition of 0.63V. [d]E_{0-0} was estimated from the absorption thresholds of dyes adsorbed on 3 μm TiO_2 film, LUMO estimated by equation of LUMO = HOMO - E_{0-0}.

Fig. 2a depicted the UV-vis absorption spectra of **D1**, **D2** and **D3** in CH_2Cl_2 solution (3×10^{-5} M), and the corresponding spectral parameters were summarized in Table 1. All three dyes presented two similar absorption bands. The short wavelength band around 340 nm could be ascribed to π–π* transition, while the long wavelength band at 500 nm was owing to the ICT transitions. Besides, upon insertion of triple bond to the neighboring donor, **D2** exhibited a slight hypochromatic shift in absorption band with respect to **D1**. Remarkably, when incorporating an ethynyl unit to the right side of auxiliary group, dye **D3** exhibited a significant redshift from 484 to 508 nm in absorption band, along with an obvious increment in molar extinction coefficient (2.57×10^4 M^{-1} cm^{-1} at 508 nm). Obviously, inserting an ethynyl unit to the side of anchoring group could obtain higher molar extinction coefficient with red shift in absorption band.

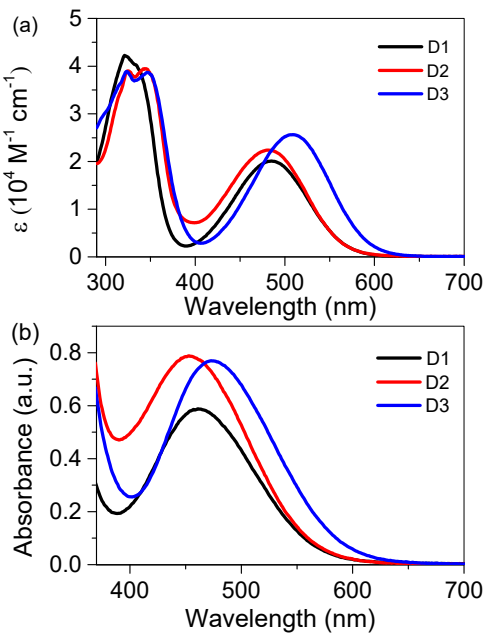

Fig. 2 Absorption spectra of dyes **D1**, **D2** and **D3** in CH_2Cl_2 solution (3×10^{-5} M, a) and anchored on 3 μm TiO_2 film (b).

Upon adsorption onto a 3 μm transparent nanocrystalline TiO_2 films, the absorption spectra of all organic dyes (Fig. 2b) were obviously hypsochromic shifted than those in solution due to the intermolecular interaction and deprotonation of carboxylic acid. The ICT bands of dyes **D1**, **D2** and **D3** showed hypsochromic shift by 22, 29 and 34 nm, respectively. Besides, **D2** and **D3** exhibit higher and broader absorption spectra compared to **D1**, indicating that the insertion of an ethynyl unit is beneficial to prolong conjugation and improve light-harvesting capability after anchoring onto TiO_2 films.

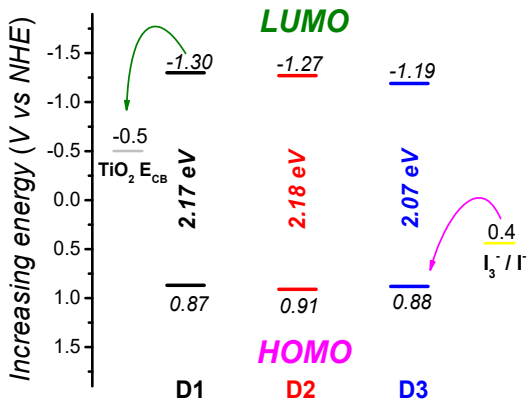

Fig. 3 Schematic diagram of the energy levels of TiO_2 conduction band, dyes **D1**, **D2** and **D3**, and iodine redox couple.

To evaluate the process of electron injection from the excited dye to the conduction band of TiO_2 and explore the ability of dye regeneration, cyclic voltammetry of three organic dyes in a typical three-electrode electrochemical cell were carried out to investigate the highest occupied molecular orbital (HOMO) energy levels (Fig. S1†). The calculated HOMO level of dye **D1** obtained from the first oxidation potentials is 0.87 V *vs.* NHE (Fig. 3). After incorporating the ethynyl unit, the HOMO level of **D2** and **D3** were both slightly shifted downward to 0.91 and 0.88 V, which were obviously lying below the iodide/triiodide (0.40 V *vs.* NHE), guaranteeing the efficient dye regeneration. The band gap energies (E_{0-0}) were estimated from the wavelength at 10% maximum absorption intensity as shown in Table 1. Interestingly, changing the ethynyl position from donor side to acceptor side leads to a narrower band gap of **D3** (2.07 V) than **D2** (2.18 V). Herein, the calculated LUMO levels of **D3** was -1.19 V, showing a relatively downward compared to **D1** (-1.30 V) and **D2** (-1.27 V). Besides, all of the

LUMO levels can guarantee the ample electron injection from the excited dyes into the TiO_2 conduction band (-0.50 V vs NHE).

To take insight into the effect of ethynyl unit to the molecular structure and electron distribution, the density functional theory (DFT) calculations of all three dyes were resorted to optimize the ground state geometries of the molecules, using the hybrid B3LYP functional[39] and the 6-31G(d) basis set (Tables S1 and S2†).[40] All calculations were carried out using the Gaussian09 program package[41]. As shown in Fig. 4, the dihedral angles between donor and auxiliary group (α) and between auxiliary group and phenyl unit (β) of three dyes exhibited definitely different values, indicative of a good molecular planarity. For dye **D1**, both of the dihedral angles possess the largest values of 33.5° and 35.5°. With insertion of triple bond to the neighboring donor, the corresponding dihedral angle of α was 0.7°, distinctly becoming planar at the side of donor compared to **D1**. Accordingly, the molecular structure of **D3** showed similar change, leading to a nearly 0° dihedral angle of β upon incorporating the ethynyl unit to the neighboring side of anchoring group. In addition, the computed spatial distribution of the frontier molecular orbitals also shows the insertion influence of ethynyl unit. It is found that both HOMO and LUMO of **D2** receive certain contributions to the ethynyl moiety, as well as that of **D3**. This change in electron distribution is beneficial to the transition process from HOMO to LUMO.

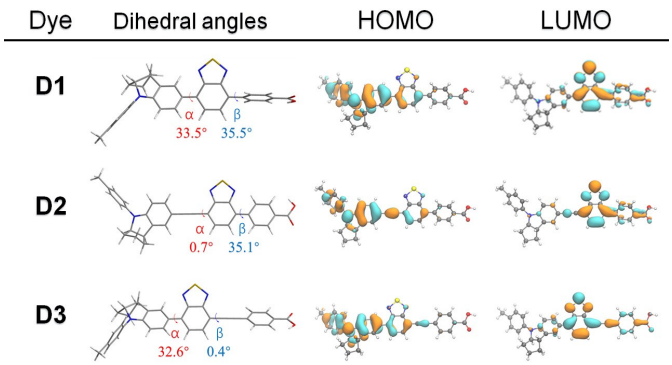

Fig. 4 Dihedral angles and Contour plots of frontier molecular orbitals of dye **D1**, **D2** and **D3**.

The photocurrent–voltage (*I*–*V*) curves of DSSCs based on three dyes were measured under an irradiance of simulated AM1.5G sunlight (100 mW cm^{-2}) using iodide/triiodide electrolyte (Fig. 5a), and the relevant parameters are summarized in Table 2. **D1** based DSSCs performed an efficiency (η) of 6.12%, with a short-circuit current (J_{SC}) of 12.6 mA cm^{-2}, an open-circuit voltage (V_{OC}) of 728 mV and a fill factor (*FF*) of 0.67. As expected, the slightly higher J_{SC} values of 13.22 and 13.44 mA cm^{-2} were obtained with dyes **D2** and **D3** than that of **D1**, probably due to the larger conjugation in molecular structure upon inserting ethynyl unit. As shown in the incident photon-to-current conversion efficiency (IPCE) spectra (Fig. 5b), **D2** and **D3** exhibited slightly broader plateau than that of **D1**, along with no obvious change of the initial response wavelength. Besides, **D3** achieved over 70% in the range of 440-600 nm, with a highest IPCE value of 80% at 480 nm. As a consequence, the improvement in J_{SC} of **D2** and **D3** could be attributed to the broader absorption spectra and the enhanced absorption coefficients.

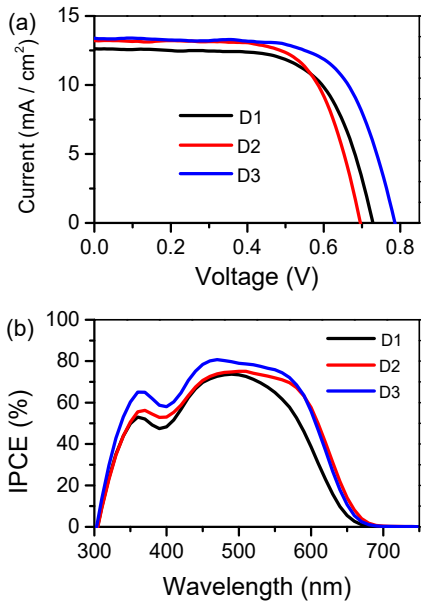

Fig. 5 *I-V* curves (a) and IPCE spectra (b) for the DSSCs fabricated on dyes **D1**, **D2**, and **D3** obtained under AM 1.5G simulated solar light (100 mW cm^{-2}).

Moreover, with insertion of triple bond to the side of anchoring group, the DSSCs based on **D3** brought forth a distinct increase of 91 mV in V_{OC} value than that of **D2**, which incorporated ethynyl unit to the side of donor, resulting in a relatively higher efficiency of 7.13%. It should be noted that, with a little change in molecular engineering, the DSSCs based **D3** obtained a predominant contribution from the enhancement in V_{OC} compared to that of **D2**.

Table 2 Photovoltaic parameters of DSSCs based on dyes **D1**, **D2** and **D3**.

Conditions	J_{SC} (mA cm^{-2})	V_{OC} (mV)	FF	η (%)	Amount of dye molecular / mol cm^{-2}
D1	12.61	728	0.667	6.12	1.55×10^{-7}
D2	13.22	695	0.683	6.28	2.58×10^{-7}
D3	13.44	786	0.675	7.13	2.33×10^{-7}

As well known, the variation of V_{OC} is dependent upon the position of TiO_2 conduction band (E_{CB}) and the electron density in the semiconductor. The electron density is strongly on account of the rate of charge recombination, which can usually evaluated by the electron lifetimes. To analysis the variances of three dye-based sensitizers in the voltage as well as further investigate interfacial charge transfer and recombination process, we performed electrochemical impedance analysis (EIS) in the dark with a series of bias voltage. The values of

View Article Online
DOI: 10.1039/C6TC03418C

chemical capacitance (C_μ) of these identical devices were shown in Fig. 6a, which is relevant to the shift of conduction band of TiO_2. It could be found that for all three dyes, the logarithm of C_μ increases linearly with the bias voltage in the same order of magnitude. Here, the same level C_μ values meant that the positions of TiO_2 conduction band of **D2** and **D3** based sensitizers were little fluctuation after inserting the ethynyl unit compared to that of **D1**.

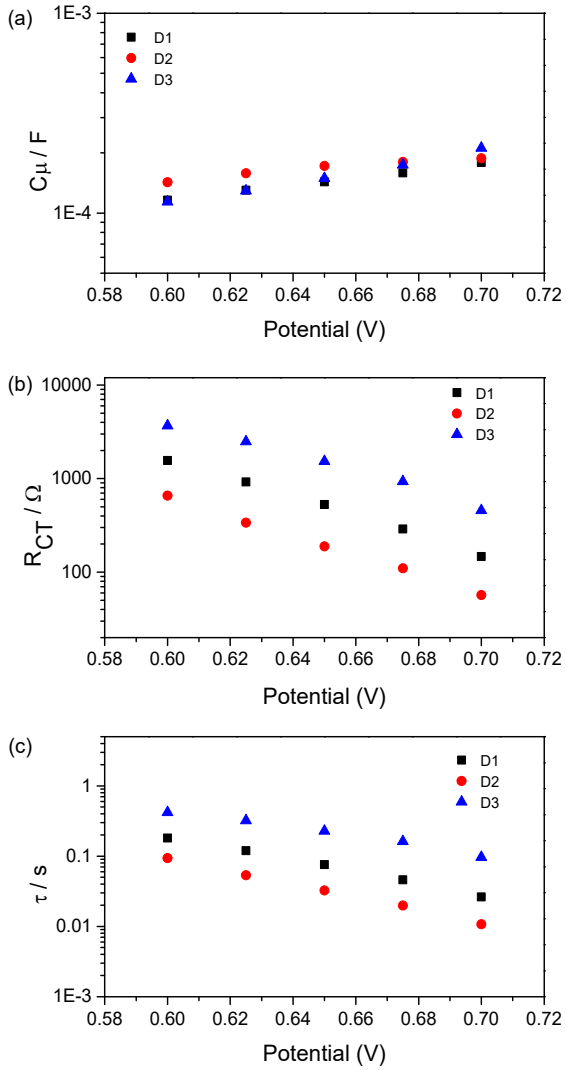

Fig. 6 TiO_2 capacitance (a), recombination resistance (b), and calculated electron lifetime (c) as a function potential based on **D1**, **D2** and **D3**.

On the other hand, the recombination resistance (R_{CT}) of all three sensitizers are presented in Fig. 6b. At a fixed potential, the R_{CT} increased as **D2** < **D1** < **D3**, which were in great agreement with their relevant tendency of V_{OC} values. The electron lifetimes as a function of potential were also measured to further elucidate the degree of electron recombination at the TiO_2 electrolyte interface, which could be obtained from the equation of $\tau = C_\mu R_{CT}$. As shown in Fig. 6c, **D3** based DSSCs exhibited longer lifetime in all region of tested potential than that of **D2**, which implies that the insertion of ethynyl unit to the neighboring side of anchoring group can more effectively suppress the process of charge recombination, resulting in obviously higher electron density in TiO_2 conduction band. As a result, it renders the superior photovoltage performance of **D3** based cells. Generally speaking, after inserting an ethynyl group on the side of anchoring group, **D3** exhibited extraordinary open circuit voltage than **D1** and **D2**, which can be an effective method to improve solar cell performance in future design. Herein, the HOMO levels may not be the major reason inducing the variation of VOC.

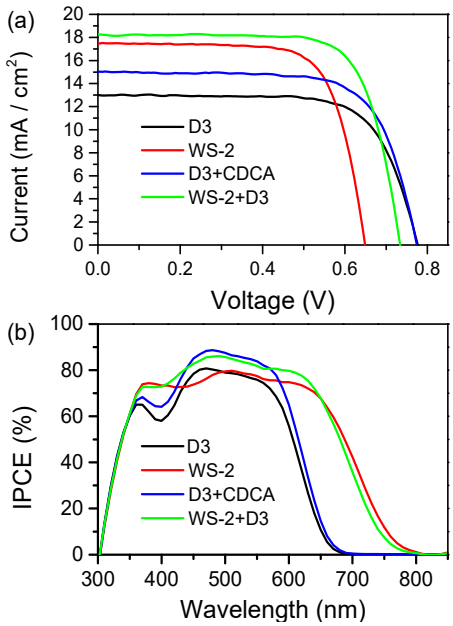

Fig. 7 *I-V* plots for DSSCs based on **D3**, **D3**+CDCA, and **WS-2**+**D3** (a), IPCE spectra for DSSCs based on **D3**, **WS-2**, **D3**+CDCA, **WS-2**+**D3** (b)

As mentioned above, **D3** showed a narrow IPCE response leading to a low J_{SC} values along with the cutoff wavelength at 700 nm, and a moderate dip in the IPCE spectrum is observed around 400 nm, which is mainly resulted from the effects of the low absorbance of dyes in this region and the competitive absorption of triiodide in the electrolyte. Given that **D3** exhibited a potentially high photvoltage, **D3** based DSSCs is expected to be optimized when the IPCE spectrum would be improved, especially at long wavelength region. We further exploited chenodeoxycholic acid (CDCA) as a coadsorbent with **D3** to improve the photovoltaic performance. Indeed, the relevant solar cells achieved higher J_{SC} with a slight decrease of V_{OC}, resulting in a higher efficiency of 8.22% (V_{OC}: 775 mV; J_{SC}: 15.1 mA cm^{-2}). Its IPCE spectrum also showed an obvious increment in the range of 350-630 nm compared to individual dye (Fig. 7b). This improvement could be attributed to the influence of CDCA, which can reduce the dye aggregation and the intermolecular interaction to some extent. Besides, the amount of adsorbed **D3** almost has no significant change after coadsorption with CDCA (Table 3).

View Article Online
DOI: 10.1039/C6TC03418C

Table 3 Photovoltaic parameters of DSSCs based on **D3+CDCA**, **WS-2+D3** and **WS-2**.

Conditions	J_{SC} (mA cm^{-2})	V_{OC} (mV)	*FF*	*η* (%)	Amount of dye molecular/ mol cm^{-2}
D3+CDCA	15.06	775	0.704	8.21	2.32×10^{-7}
WS-2+D3	18.30	737	0.729	9.83	$0.45\times10^{-7}+1.87\times10^{-7}$
WS-2	17.51	649	0.720	8.18	2.10×10^{-7}

Although the utilization of CDCA can improve the cell performance by suppressing dye aggregations, there is no dramatic promotion in photovoltaic efficiency, especially the relatively narrow IPCE response still restricted the performances of **D3**-based solar cells. Here, another strategy of cosensitization with a broad spectral response dye for pursuing better cell performances was carried out. According to our previous work, **WS-2** (Fig. S2†)[33c] exhibited efficient IPCE values above 70% from 400 to 680 nm with the cutoff wavelength at 800 nm, which is apparently compensated with dye **D3**. Besides, **D3** showed an extremely high open-circuit voltage, which can well improve the poor performance in photovoltage of **WS-2**.

For the cosensitized cells of **WS-2** and **D3**, the IPCE spectra showed above 80% from 450 to 650 nm with the cutoff wavelength extending to 800 nm. The adsorption amount for **WS-2** and **D3** in the cosensitized condition are 0.45×10^{-7} and 1.87×10^{-7} mol cm^{-2}, respectively. After cosensitization, the amount of **D3** decreased from 2.33×10^{-7} to 1.87×10^{-7} mol cm^{-2}, but a considerable amount of **WS-2** was adsorbed, which resulted in a significant enhancement in IPCE spectra. Furthermore, the V_{OC} of cosensitized cells became 737 mV, an obvious increase relative to the single **WS-2** (653 mV). Finally, as shown in Fig. 7a and Table 3, the strategy of cosensitization with **WS-2** resulted in a significant enhancement in J_{SC}, and showed an excellent efficiency of 9.83% in the iodine electrolyte.

Conclusions

In summary, we have synthesized three novel D-A-π-A featured organic dyes, and taken systematic insight into the effect of ethynyl positions on photovoltaic performances. Compared to **D1**, dye **D2** incorporating an ethynyl group between the donor group indoline and auxiliary group showed little change to absorption and limited enhancement in molar extinction coefficients, eventually had no significant promotion in photovoltaic performance. However, upon inserting an ethynyl group between the auxiliary group and benzene ring, dye **D3** successfully red-shifted the absorption band, and enhanced the molar extinction coefficients, finally achieving a better efficiency of 7.13%. Strikingly, **D3** exhibited excellent V_{OC} values (786 mV) than **D1** and **D2**, indicating that this triple bond position could effectively retard the electron recapture, which was proved by measurements of EIS. The addition of coadsorbent CDCA with dye **D3** exhibited dramatically higher J_{SC} values, resulting in a performance of 8.22%. The cosensitization strategy of **WS-2/D3** also achieved an obvious enhancement compared to individual dye, reaching an optimized efficiency of 9.83% (J_{SC} = 18.30 mA cm^{-2}, V_{OC} = 737 mV, and *FF* = 0.73). Our results indicate that insertion of an ethynyl group to the proper position can effectively broaden the spectra response and develop high efficient D-A-π-A organic sensitizers, paving a practically molecular engineering in development of D-A-π-A featured metal-free organic dyes.

Acknowledgements

This work was supported by NSFC for Creative Research Groups (21421004) and Distinguished Young Scholars (21325625), NSFC/China, Oriental Scholarship, Fundamental Research Funds for the Central Universities (WJ1416005), Scientific Committee of Shanghai (15XD1501400), and Programme of Introducing Talents of Discipline to Universities (B16017).

Notes and references

1 (*a*) B. O'Regan and M. Gratzel, *Nature*, 1991, **353**, 737; (*b*) A. Hagfeldt, G. Boschloo, L. Sun, L. Kloo and H. Pettersson, *Chem. Rev.*, 2010, **110**, 6595; (*c*) Y. Lin, Y. Li and X. Zhan, *Chem. Soc. Rev.*, 2012, **41**, 4245; (*d*) Z. He, C. Zhong, X. Huang, W. Wong, H. Wu, L. Chen, S. Su and Y. Cao, *Adv. Mater.*, 2011, **23**, 4636.
2 (*a*) S. Zhang, X. Yang, Y. Numata and L. Han, *Energy Environ. Sci.*, 2013, **6**, 1443; (*b*) Z. Ning, Y. Fu and H. Tian, *Energy Environ. Sci.*, 2010, **3**, 1170; (*c*) Y. F. Li, *Sci. China Chem.*, 2015, **58**, 830.
3 (*a*) Y. Z. Wu, W. H. Zhu, S. M. Zakeeruddin and M. Grätzel, *ACS Appl. Mater. Interfaces*, 2015, **7**, 9307; (*b*) L. L. Li and E. W. G. Diau, *Chem. Soc. Rev.*, 2013, **42**, 291; (*c*) I. Chung, B. Lee, J. He, R. P. H. Chang and M. G. Kanatzidis, *Nature*, 2012, **485**, 486; (*d*) G. Calogero, A. Bartolotta, G. D. Marco, A. D. Carlo and F. Bonaccorso, *Chem. Soc. Rev.*, 2015, **44**, 3244; (*e*) C. P. Lee, R. Y. Lin, L. Y. Lin, C. Li, T. Chu, S. Sun, J. T. Lin and K. Ho, *RSC Adv.*, 2015, **5**, 23810.
4 K. Kakiage, Y. Aoyama, T. Yano, K. Oya, J. Fujisawa and M. Hanaya, *Chem. Commun.*, 2015, **51**, 15894.
5 N. Robertson, *Angew. Chem., Int. Ed.*, 2006, **45**, 2338.
6 T. Higashino, Y. Fujimori, K. Sugiura, Y. Tsuji, S. Ito and H. Imahori, *Angew. Chem., Int. Ed.*, 2015, **54**, 9052.
7 (*a*) Y. Hu, A. Ivaturi, M. Planells, C. L. Boldrini, A. O. Biroli and N. Robertson, *J. Mater. Chem. A*, 2016, **4**, 2509.
8 S. Yun, P. D. Lund and A. Hinsch, *Energy Environ. Sci.*, 2015, **8**, 3495.
9 (*a*) H. Jia, M. Zhang, W. Yan, X. Ju and H. Zheng, *J. Mater. Chem. A*, 2016; (*b*) J. Ni, Y. Yen and J. T. Lin, *J. Mater. Chem. A*, 2016, **4**, 6553; (*c*) S. Chaurasia, C. Liang, Y. Yen and J. T. Lin, *J. Mater. Chem. C.*, 2015, **3**, 9765; (*d*) H. Chou, Y. Chen, H. Huang, T. Lee, J. T. Lin, C. Tsai and K. Chen, *J. Mater. Chem.*, 2012, **22**, 10929; (*e*) C. Du, L. Jiang, L. Sun, N. Huang and W. Deng, *RSC Adv.*, 2015, **5**, 37574.
10 (*a*) W. Zhang, Y. Z. Wu, H. Zhu, Q. Chai, J. Liu, H. Li, X. Song and W. H. Zhu, *ACS Appl. Mater. Interfaces*, 2015, **7**, 26802; (*b*) B. Liu, B. Wang, R. Wang, L. Gao, S. Huo, Q. Liu, X. Li and W. H. Zhu, *J. Mater. Chem. A*, 2013, **2**, 804.
11 S. Li, K. Jiang, K. Shao and L. Yang, *Chem. Commun.*, 2006, 2792.

12 (*a*) J. Yang, P. Ganesan, J. Teuscher, T. Moehl, Y. J. Kim, C. Yi, P. Comte, K. Pei, T. W. Holcombe, M. K. Nazeeruddin, J. Hua, S. M. Zakeeruddin, H. Tian and M. Grätzel, *J. Am. Chem. Soc.*, 2014, **136**, 5722. (*b*) J. Shi, Z. F. Chai, R. L. Tang, J. L. Hua, Q. Q. Li and Z. Li, *Sci. China: Chem.*, 2015, **58**, 1144; (*c*) X. Li, Y. Hu, I. Sanchez-Molina, Y. Zhou, F. Yu, S. A. Haque, W. Wu, J. Hua, H. Tian and N. Robertson, *J. Mater. Chem. A*, 2015, **3**, 21733.

13 (*a*) Z. S. Huang, H. Meier and D. Cao, *J. Mater. Chem. C*, 2016, **4**, 2404; (*b*) Z. S. Huang, X. Zang, T. Hua, L. Wang, H. Meier and D. Cao, *ACS Appl. Mater. Interfaces*, 2015, **7**, 20418.

14 (*a*) Y. K. Eom, S. H. Kang, I. T. Choi, E. Kim, J. Kim, M. J. Ju and H. K. Kim, *RSC Adv.*, 2015, **5**, 80859; (*b*) Y. J. Chang, M. Watanabe, P. Chou and T. J. Chow, *Chem. Commun.*, 2012, **48**, 726.

15 N. J. Zhou, K. Prabakaran, B. Lee, S. H. Chang, B. Harutyunyan, P. J. Guo, M. R. Butler, A. Timalsina, M. J. Bedzyk, M. A. Ratner, S. Vegiraju, S. Yau, C. G. Wu, R. P. H. Chang, A. Facchetti, M. C. Chen and T. J. Marks, *J. Am. Chem. Soc.*, 2015, **137**, 4414.

16 (*a*) H. Choi, M. Shin, K. Song, M. Kang, Y. Kang and J. Ko, *J. Mater. Chem. A*, 2014, **2**, 12931; (*b*) D. Joly, L. Pellejà, S. Narbey, F. Oswald, J. Chiron, J. N. Clifford, E. Palomares and R. Demadrille, *Sci. Rep.*, 2014, **4**, 4033; (*c*) D. Joly, L. Pelleja, S. Narbey, F. Oswald, T. Meyer, Y. Kervella, P. Maldivi, J. N. Clifford, E. Palomares and R. Demadrille, *Energy Environ. Sci.*, 2015, **8**, 2010.

17 (*a*) X. Xu, H. Wang, F. Gong, G. Zhou and Z. S. Wang, *ACS Appl. Mater. Interfaces*, 2013, **5**, 3219; (*b*) J. Wu, G. Li, L. Zhang, G. Zhou and Z. S. Wang, *J. Mater. Chem. A*, 2016, **4**, 3342.

18 Z. Wang, M. Liang, Y. Tan, L. Ouyang, Z. Sun and S. Xue, *J. Mater. Chem. A*, 2015, **3**, 4865.

19 T. Marinado, K. Nonomura, J. Nissfolk, M. K. Karlsson, D. P. Hagberg, L. Sun, S. Mori and A. Hagfeldt, *Langmuir*, 2009, **26**, 2592.

20 X. Qian, Y. Zhu, W. Chang, J. Song, B. Pan, L. Lu, H. Gao and J. Zheng, *ACS Appl. Mater. Interfaces*, 2015, **7**, 9015.

21 (*a*) H. Ellis, I. Schmidt, A. Hagfeldt, G. Wittstock and G. Boschloo, *J. Phys. Chem. C*, 2015, **119**, 21775; (*b*) H. Tian, X. Yang, R. Chen, A. Hagfeldt and L. Sun, *Energy Environ. Sci.*, 2009, **2**, 674.

22 S. Mathew, A. Yella, P. Gao, R. Humphry-Baker, B. F. E. Curchod, N. Ashari-Astani, I. Tavernelli, U. Rothlisberger, M. K. Nazeeruddin and M. Grätzel, *Nat. Chem.*, 2014, **6**, 242.

23 A. Yella, H. W. Lee, H. N. Tsao, C. Yi, A. K. Chandiran, M. K. Nazeeruddin, E. W. G. Diau, C. Y. Yeh, S. M. Zakeeruddin and M. Grätzel, *Science*, 2011, **334**, 629.

24 (*a*) C. Chou, F. Hu, H. Yeh, H. Wu, Y. Chi, J. N. Clifford, E. Palomares, S. Liu, P. Chou and G. Lee, *Angew. Chem., Int. Ed.,* 2014, **53**, 178; (*b*) A. Broggi, I. Tomasi, L. Bianchi, A. Marrocchi and L. Vaccaro, *ChemPlusChem*, 2014, **79**, 486; (*c*) C. Zhang, L. Wang, W. Tan, S. Wu, X. Liu, P. Yu, J. Huang, X. Zhu, H. Wu, C. Zhao, J. Peng and Y. Cao, *J. Mater. Chem. C.*, 2016, **4**, 3757.

25 A. Yella, C. Mai, S. M. Zakeeruddin, S. Chang, C. Hsieh, C. Yeh and M. Grätzel, *Angew. Chem., Int. Ed.,* 2014, **126**, 3017.

26 Z. Yao, M. Zhang, H. Wu, L. Yang, R. Li and P. Wang, *J. Am. Chem. Soc.*, 2015, **137**, 3799.

27 (*a*)Y. Xie, Y. Tang, W. Wu, Y. Wang, J. Liu, X. Li, H. Tian and W. H. Zhu, *J. Am. Chem. Soc.*, 2015, **137**, 14055; (*b*) Y. Wang, B. Chen, W. Wu, X. Li, W. H. Zhu, H. Tian and Y. Xie, *Angew. Chem., Int. Ed.*, 2014, **53**, 10779.

28 C. Wang, J. Hu, C. Wu, H. Kuo, Y. Chang, Z. Lan, H. Wu, E. W. G. Diau and C. Lin, *Energy Environ. Sci.*, 2014, **7**, 1392.

29 (*a*) J. Luo, M. Xu, R. Li, K. Huang, C. Jiang, Q. Qi, W. Zeng, J. Zhang, C. Chi, P. Wang and J. Wu, *J. Am. Chem. Soc.*, 2013, **136**, 265; (*b*) Q. Qi, X. Wang, L. Fan, B. Zheng, W. Zeng, J. Luo, K. Huang, Q. Wang and J. Wu, *Org. Lett.*, 2015, **17**, 724.

30 L. Pellejà, C. V. Kumar, J. N. Clifford and E. Palomares, *J. Phys. Chem. C*, 2014, **118**, 16504.

31 C. Hsieh, H. Lu, C. Chiu, C. Lee, S. Chuang, C. Mai, W. Yen, S. Hsu, E. W. G. Diau and C. Yeh, *J. Mater. Chem.*, 2010, **20**, 1127.

32 (*a*) H. Wu, L. Yang, Y. Li, M. Zhang, J. Zhang, Y. Guo and P. Wang, *J. Mater. Chem. A*, 2016, **4**, 519; (*b*) C. Yan, W. Ma, Y. Ren, M. Zhang and P. Wang, *ACS Appl. Mater. Interfaces*, 2015, **7**, 801.

33 (*a*) Y. Z. Wu and W. H. Zhu, *Chem. Soc. Rev.*, 2013, **42**, 2039; (*b*) X. Kang, J. Zhang, D. O'Neil, A. J. Rojas, W. Chen, P. Szymanski, S. R. Marder and M. A. El-Sayed, *Chem. Mater.*, 2014, **26**, 4486; (*c*) W. H. Zhu, Y. Z. Wu, S. Wang, W. Li, X. Li, J. Chen, Z. S. Wang and H. Tian, *Adv. Funct. Mater.*, 2011, **21**, 756; (*d*) X. Kang, J. Zhang, A. J. Rojas, D. O'Neil, P. Szymanski, S. R. Marder and M. A. El-Sayed, *J. Mater. Chem. A*, 2014, **2**, 11229.

34 J. Shiu, Y. Chang, C. Chan, H. Wu, H. Hsu, C. Wang, C. Lin and E. W. Diau, *J. Mater. Chem. A*, 2015, **3**, 1417.

35 (*a*) K. Pei, Y. Z. Wu, H. Li, Z. Geng, H. Tian and W. H. Zhu, *ACS Appl. Mater. Interfaces*, 2015, **7**, 5296; (*b*) J. Liu, B. Liu, Y. Tang, W. Zhang, W. Wu, Y. Xie and W. H. Zhu, *J. Mater. Chem. C*, 2015, **3**, 11144; (c) W. Zhang, W. Li, Y. Z. Wu, J. Liu, X. Song, H. Tian and W. H. Zhu, *ACS Sustainable Chem. Eng.*, 2016, **4**, 3567.

36 (*a*) S. Zhang, A. Islam, X. Yang, C. Qin, K. Zhang, Y. Numata, H. Chen and L. Han, *J. Mater. Chem. A*, 2013, **1**, 4812; (*b*) Y. Numata, S. Zhang, X. Yang and L. Han, *Chem. Lett.*, 2013, **42**, 1328.

37 B. Hardin, A. Sellinger, T. Moehl, R. Humphry-Baker, J. Moser, P. Wang, S. M. Zakeeruddin, M. Grätzel, and M. D. McGehee, *J. Am. Chem. Soc.*, 2011, **133**, 10662.

38 L. Han, A. Islam, H. Chen, C. Malapaka, B. Chiranjeevi, S. Zhang, X. Yang and M. Yanagida, *Energy Environ. Sci.*, 2012, **5**, 6057.

39 A. D. Becke, *J. Chem. Phys.*, 1993, **98**, 5648.

40 W. J. Hehre, R. Ditchfield and J. A. Pople, *J. Chem. Phys.*, 1972, **56**, 2257.

41 M. J. Frisch, G. W. Trucks, H. B. Schlegel, P. M. W. Gill, B. G. Johnson, M. A. Robb, J. R. Cheeseman, T. Keith, G. A. Petersson, J. A. Montgomery, K. Raghavachari, M. A. Al-Laham, V. G. Zakrzewski, J. V. Ortiz, J. B. Foresman, J. Cioslowski, B. B. Stefanov, A. Nanayakkara, M. Challacombe, C. Y. Peng, P. Y. Ayala, W. Chen, M. W. Wong, J. L. Andres, E. S. Replogle, R. Gomperts, R. L. Martin, D. J. Fox, J. S. Binkley, D. J. Defrees, J. Baker, J. P. Stewart, M. Head-Gordon, C. Gonzalez and J. A. Pople, *Gaussian 03*, *revision C.01*, *Gaussian*, Inc., Pittsburgh, PA, 2004.

View Article Online
DOI: 10.1039/C6TC03418G

Influence of ethynyl position on benzothiadiazole based D-A-π-A dye-sensitized solar cells: spectral response and photovoltage performance

Xiongrong Song, Weiwei Zhang, Xin Li, Huiyun Jiang, Chao Shen and Wei-Hong Zhu*

Three novel D-A-π-A featured organic dyes has been designed for systematic insight into the effect of ethynyl positions on photovoltaic performances. Insertion of triple bond close to anchoring group exhibits better photovoltaic performance with strikingly higher open-circuit voltage. With the efficient cosensitization method, the optimized device achieved an excellent efficiency of 9.83%.